SUPPLEMENTARY INFORMATION

Relaxation Dynamics of *Pseudomonas aeruginosa* Re^I(CO)$_3$(α-diimine)(HisX)$^+$ (X = 83, 107, 109, 124, 126)Cu^{II} Azurins

Ana María Blanco-Rodríguez,[a] Michael Busby,[a] Kate Ronayne,[b] Michael Towrie,[b] Cristian Grădinaru,[c] Jawahar Sudhamsu,[c] Jan Sýkora,[d] Martin Hof,[d] Stanislav Záliš,[d] Angel J. Di Bilio,[e] Brian R. Crane,*[c] Harry B. Gray*[e], Antonín Vlček, Jr.*[a,d]

[a] School of Biological and Chemical Sciences, Queen Mary, University of London, Mile End Road, London E1 4NS, United Kingdom

[b] Central Laser Facility, CCLRC Rutherford Appleton Laboratory, Chilton, Didcot, Oxfordshire OX11 0QX, United Kingdom,

[c] Department of Chemistry and Chemical Biology, Cornell University, Ithaca, New York 14853, USA

[d] J. Heyrovský Institute of Physical Chemistry, Academy of Sciences of the Czech Republic, Dolejškova 3, 182 23 Prague, Czech Republic

[e] Beckman Institute, California Institute of Technology, Pasadena, CA 91125, USA

E-mail: a.vlcek@qmul.ac.uk, bc69@cornell.edu, hbgray@ caltech.edu

Tables

Table S1. Angles between the project of the N$^\varepsilon$-C$^{\varepsilon1}$ (the C atom between the two imidazole nitrogens) of the his imidazole into the Re(CO)$_2$(N,N) plane and the line bisecting the angle between the two equatorial carbonyls. (Angle of 0 ° corresponds to C$^{\varepsilon1}$ lying in the symmetry plane of the Re(CO)$_2$(N,N) moiety, pointing between the carbonyls.) Values are in degrees.

Re-azurin	angle for each unique molecule in the asymmetric unit			
83-phen	3	355		
124-phen	35	93		
107-dmp	261	130		
109-phen	286[a]	93[a]	260[b]	78[b]
126phen	281	279	129	280

[a,b] Data correspond to the two **109-phen** isomers.

Table S2. DFT (PBE0/CPCM-H$_2$O) calculated spectroscopically relevant Kohn-Sham molecular orbitals of **Re(Etim)**, conformation A.

MO	E (eV)	Prevailing character	Re	phen	CO$_{ax}$	2CO$_{eq}$	Etim
Unoccupied							
105a	-0.80	Re + CO	31	5	16	47	1
104a	-1.02	$\pi*$ phen	2	92	0	5	1
103a	-2.22	$\pi*$ phen	0	99	0	0	0
102a	-2.49	$\pi*$ phen	3	93	0	4	1
Occupied							
101a	-6.66	Re	45	11	9	10	25
100a	-6.83	Re	62	8	13	13	4
99a	-7.06	Re + Et-im	32	4	1	13	50
98a	-7.12	Re	47	4	2	19	27
97a	-7.49	π phen	7	86	1	1	4
96a	-7.82	phen	2	98	0	0	0

Table S3. DFT (PBE0/CPCM-H$_2$O) calculated spectroscopically relevant Kohn-Sham molecular orbitals of **Re(Etim)**, conformation B.[a]

MO	E (eV)	Prevailing character	Re	phen	CO$_{ax}$	2CO$_{eq}$	Etim
Unoccupied							
105a	-0.83	Re + CO	28	5	16	43	7
104a	-1.05	$\pi*$ phen	2	91	0	5	1
103a	-2.24	$\pi*$ phen	1	99	0	1	0
102a	-2.51	$\pi*$ phen	3	93	0	3	1
Occupied							
101a	-6.64	Re	54	4	13	12	16
100a	-6.87	Re	55	21	10	13	1
99a	-7.03	Re	7	2	1	2	88
98a	-7.08	Re	64	4	1	28	3
97a	-7.55	π phen	12	83	2	2	1
96a	-7.84	π phen	1	98	0	0	1

[a] To determine the molecular structure, the angle between the im plane and the symmetry plane of the Re(CO)$_3$(phen) unit was fixed at 90° and remaining structural parameters were optimized. Full ground-state geometry optimization of B in H$_2$O did not converge.

Table S4. TD-DFT (PBE0/CPCM-H$_2$O) calculated lowest singlet electronic transitions of **Re(Etim)** (conformation B[a]) with oscillator strength larger than 0.001. (Transition energies in eV, the corresponding wavelength (nm) in parenthesis. Molar absorptivity in M^{-1}cm^{-1}) Experimental data are for **Re(im)**.[1]

State	Main components (%)	Calculated transitions	Osc. Str.	Expt. transitions	Molar abs.
b^{1}A, MLCT	90 (101a→102a)	3.32 (373)	0.073	3.40 (365)	~3500
c^{1}A, MLCT	91 (100a→102a)	3.37 (367)	0.028	3.40 (365)	~3500
d^{1}A, MLCT	92 (101a→103a)	3.66 (339)	0.024	3.76 (330)	
e^{1}A, MLCT	91 (100a→103a)	3.76 (330)	0.015	3.76 (330)	

[a] To determine the molecular structure, the angle between the im plane and the symmetry plane of the Re(CO)$_3$(phen) unit was fixed at 90° and remaining structural parameters were optimized. Full ground-state geometry optimization of B in H$_2$O did not converge.

Table S5. TD-DFT PBE0/CPCM (H$_2$O) calculated lowest singlet electronic transitions of **Re(Etim)** (conformation A) with oscillator strength larger than 0.001. (Transition energies in eV, the corresponding wavelength (nm) in parenthesis. Molar absorptivity in M^{-1}cm^{-1}) Experimental data are for **Re(im)**.[1]

State	Main components (%)	Calculated transitions	Osc. Str.	Expt. transitions	Molar abs.
b^{1}A, MLCT	99 (101a→102a)	3.17 (390)	0.002		
c^{1}A, MLCT	85 (100a→102a)	3.47 (358)	0.068	3.40 (365)	~3500
d^{1}A, MLCT	80 (101a→103a)	3.62 (342)	0.093	3.76 (330)	

Table S6. ν(CO) IR bands of **Re(Etim)** in the ground state and the lowest triplet excited state. Δ = shift of the IR band upon excitation, Values in cm^{-1}. (Δ values for the conformation B are not available since the ground-state calculation of B did not converge.)

	Ground state			Excited state				Δ		
	Exp.	Calc.[a] A-vac	Calc.[b] A-H$_2$O	Exp.	Calc[a] A-vac	Calc.[b] A-H$_2$O	Calc.[b] B-H$_2$O	Exp.	Calc.[a] A-vac	Calc.[b] A-H$_2$O
A"	1925	1920	1924	1968	1947	1977	1972	43	27	53
A'(2)	1925	1929	1925	2013	1979	2025	2014	88	50	100
A'(1)	2032	2000	2053	2072	2021	2084	2059	40	21	31

[a] *in vacuo* calculated values (scaling factor 0.9285)
[b] PBE0/CPCM-H$_2$O, calculated values (scaling factor 0.9725)

Table S7. Stretched-exponential (eq. 5) dynamic shift parameters of the A'(1) ν(CO) band of Re-azurins in KP_i (D_2O, pD ~ 7.1) buffer at 21 °C. Re-azurin concentrations are in the range 3.5-6 mM. Parameters are based on Gaussian band-shape fitting of **83-phen**, **109-phen**, **107-dmp 126-phen**, and asymmetric log-norm fitting of **124-phen**. Two sets of results are presented for **107-dmp** based on spectra obtained with 4.5-5.5 cm^{-1} resolution (LR) and 2-3 cm^{-1} resolution (HR). Kinetics fitting was begun at 2 ps, except **126-phen** that is fitted from 1 ps. Only a low-quality fit was obtained for **126-phen**.

	109[a]	83[a]	124	126	107 LR, 3-exp	107 HR
A_1	3.4±0.1	5.0±0.2	11.7±0.1	3.8±0.2	3.4±0.3	2.0±0.1
A_2	51.1±10.0	28.0±10.0	37.5±13.6	43.9±19.5	19.0±7.2	9.5±2.0
τ_1	327±25	297±36	540.6±11.4	346±61	131±24	243±38
β	0.4±0.04	0.5±0.1	0.48±0.1	0.4±0.1	0.8±0.2	0.6±0.1
τ_2	0.6±0.26	1.4±0.8	0.87±0.6	0.6±0.6	2.3±1.0	3.3±1.1

[a] Based on TRIR spectra reported before[2] which were re-fitted with Gaussian functions and tri-exponential kinetics. Therefore, the kinetics data presented herein are somewhat different from those in ref.[2] where Lorentzian fitting and bi-exponential kinetics were used.

Table S8. Dynamic shift parameters of the A'(1) ν(CO) bands of **107-dmp**, **124-phen**, and **126-phen** in KP_i (D_2O, pD ~ 7.1) buffer measured as a function of the azurin concentration at 21 °C. Parameters are based on Gaussian band-shape fitting of high-resolution TRIR spectra of **107-dmp** and **126-phen**, and asymmetric log-norm fitting (eq. 3) of high-resolution TRIR spectra of **124-phen**. Kinetics fitting was begun at 2 ps, except **126-phen** that is fitted from 1 ps.

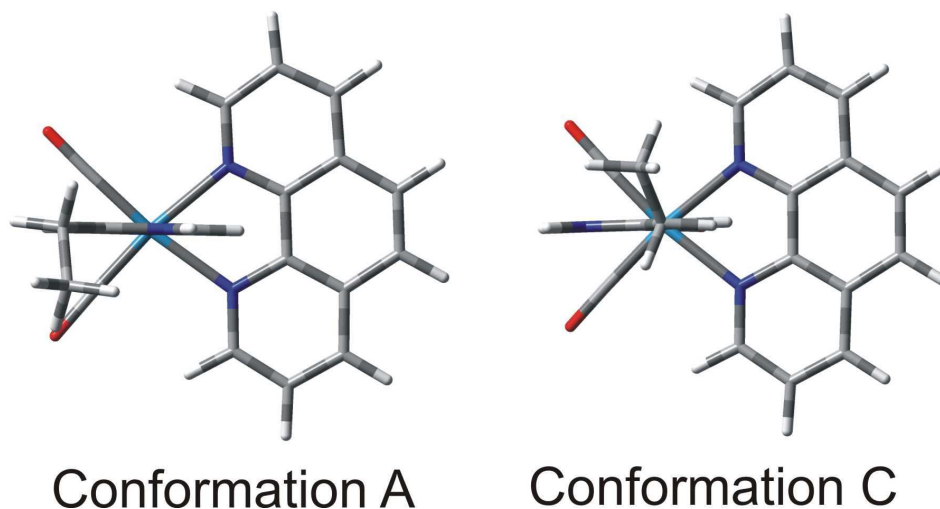|	107 5.7 mM	107 1.9 mM	107 0.5 mM	124 4.3 mm	124 1.1 mM	124 0.5 mM	126 3.5 mM	126 0.7 mM	126 0.4 mM
ν_{GS}, cm^{-1}	2028	2028	2028	2028.9	2028.9	2028.9	2030.8	2030.8	2030.3
$\nu(\infty)$, cm^{-1}	2050.1	2050.4	2051.48	2067.4	2067.19	2067.3	2066.4	2065.3	2062.6
A_1	2.0±0.1	2.2±0.1	2.5±0.1	11.7±0.1	10.9±0.1	11.0±0.2	3.8±0.2	3.4±0.2	3.0±0.3
A_2	9.5±2.0	6.2±0.7	5.2±0.6	37.5±13.6	37.2±17.0	34.6±27.2	64.8±40	102±71	37.3±17
τ_1	243±38	192±29	271±45	540.6±11.4	498.0±14.7	541.9±25.7	491±76	383±65	222±53
β	0.6±0.1	1.1±0.2	1.4±0.3	0.48±0.1	0.48±0.1	0.46±0.2	0.35±0.1	0.35±0.1	0.54±0.2
τ_2	3.3±1.1	6.1±0.6	6.7±0.7	0.87±0.6	0.90±0.7	0.86±1.3	0.26±0.4	0.16±0.3	0.97±0.8

Conformation A   Conformation C

Figure S1. DFT/PBE0 *in vacuo* optimized ground-state (a^1A) molecular structure of **Re(Etim).** The imidazole plane approximately coincides with the $Re(CO)_2(N,N)$ symmetry plane, bisecting the angle between the two equatorial carbonyls. Conformation C lies lower in energy by 0.027 eV ($\Delta G°$).
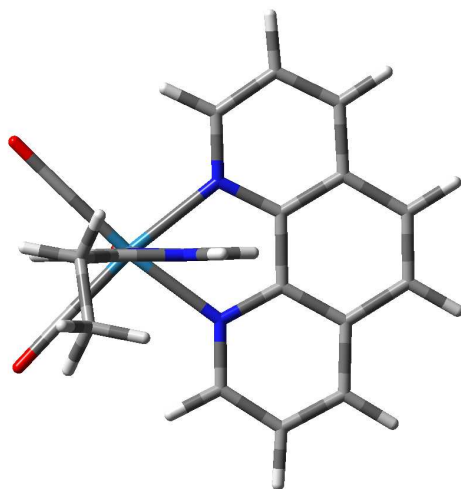

Figure S2. PBE0/CPCM-H_2O optimized ground-state (a^1A) molecular structure of **Re(Etim).** The angle between the project of the N^ε-$C^{\varepsilon 1}$ (the C atom between the two imidazole nitrogens) of the his imidazole into the $Re(CO)_2(N,N)$ plane and the line bisecting the angle between the two equatorial carbonyls is $179.0°$. No convergent solution was found for other possible conformations in H_2O.
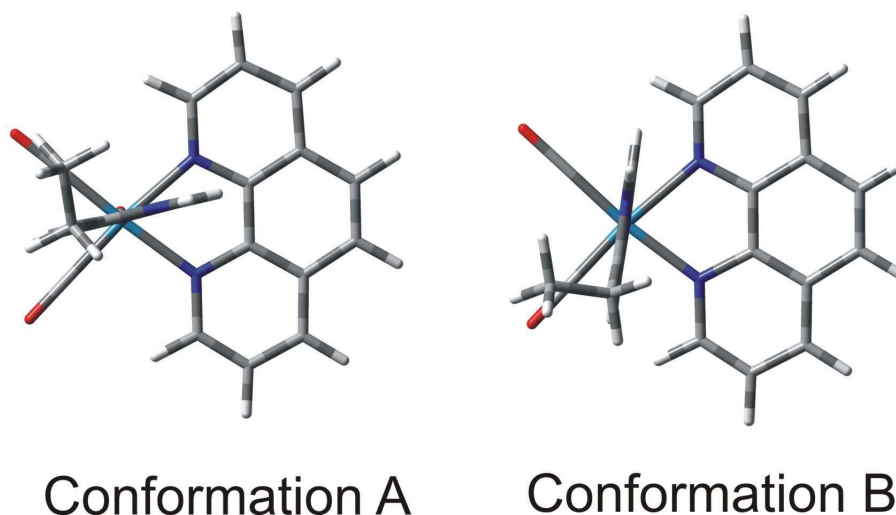
Conformation A   Conformation C

Figure S3. DFT/PBE0 *in vacuo* optimized molecular structures of the **Re(Etim)** lowest excited state a^3A (^{3}MLCT). The angles between the project of the N^ε-$C^{\varepsilon 1}$ (the C atom between the two imidazole nitrogens) of the his imidazole into the $Re(CO)_2(N,N)$ plane and the line bisecting the angle between the two equatorial carbonyls are 164.8^o and 346.0^o for conformations A and C, respectively. Conformation C lies lower in energy by 0.035 eV (ΔG°).

Conformation A   Conformation B

Figure S4. PBE0/CPCM-H$_2$O optimized molecular structures of the **Re(Etim)** lowest excited state a^3A (^{3}MLCT). The angles between the project of the N^ε-$C^{\varepsilon 1}$ (the C atom between the two imidazole nitrogens) of the his imidazole into the $Re(CO)_2(N,N)$ plane and the line bisecting the angle between the two equatorial carbonyls are 172.0^o and 96.6^o for conformations A and B, respectively. Conformation B lies lower in energy by 0.026 eV (ΔG°).
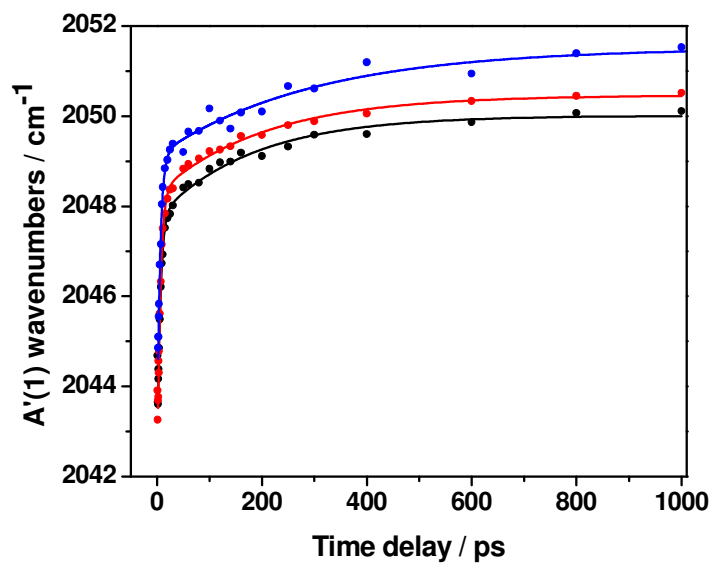
Figure S5. Time dependence of the peak energy of the A'(1) ν(CO) band of **107-dmp** measured at different concentrations: 5.7 mM (black), 1.7 mM (red), 0.5 mM (blue) The curves are the triexponential fits (eq. 1) with parameters from Table 5.
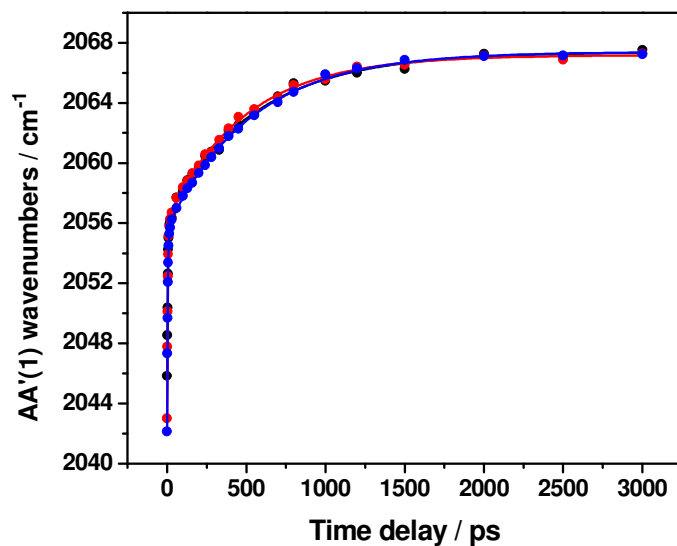

Figure S6. Time dependence of the peak energy of the A'(1) ν(CO) band of **124-phen** measured at different concentrations: 4.3 mM (blue), 1.1 mM (red), 0.5 mM (black) The curves are the triexponential fits (eq. 1) with parameters from Table 5.
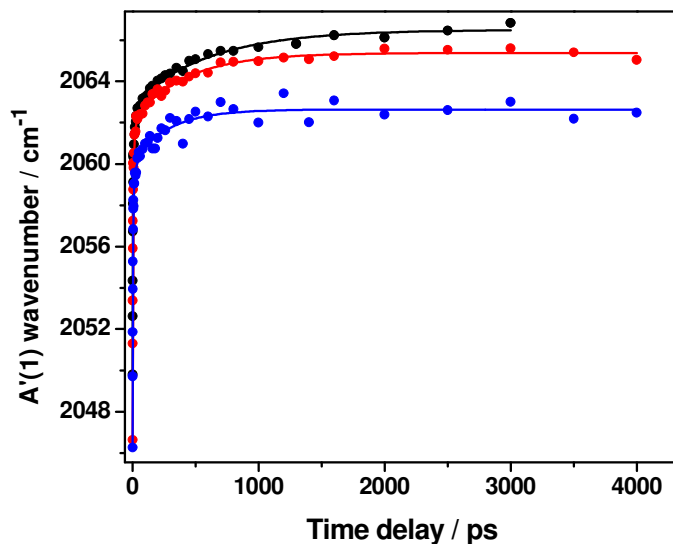
Figure S7. Time dependence of the peak energy of the A'(1) ν(CO) band of **126-phen** measured at different concentrations: 4.0 mM (black), 0.8 mM (red), 0.4 mM (blue) The curves are the triexponential fits (eq. 1) with parameters from Table 5.

References

(1) Connick, W. B.; Di Bilio, A. J.; Hill, M. G.; Winkler, J. R.; Gray, H. B. *Inorg. Chim. Acta* **1995**, *240*, 169-173.
(2) Blanco-Rodríguez, A. M.; Busby, M.; Grădinaru, C.; Crane, B. R.; Di Bilio, A. J.; Matousek, P.; Towrie, M.; Leigh, B. S.; Richards, J. H.; Vlček, A., Jr.; Gray, H. B. *J. Am. Chem. Soc.* **2006**, *128*, 4365-4370.

Full reference 33 of the main text:

Frisch, M. J.; Trucks, G. W.; Schlegel, H. B.; Scuseria, G. E.; Robb, M. A.; Cheeseman, J. R.; J. A. Montgomery, J.; Vreven, T.; Kudin, K. N.; Burant, J. C.; Millam, J. M.; Iyengar, S. S.; Tomasi, J.; Barone, V.; Mennucci, B.; Cossi, M.; Scalmani, G.; Rega, N.; Petersson, G. A.; Nakatsuji, H.; Hada, M.; Ehara, M.; Toyota, K.; Fukuda, R.; Hasegawa, J.; Ishida, M.; Nakajima, T.; Honda, Y.; Kitao, O.; Nakai, H.; Klene, M.; Li, X.; Knox, J. E.; Hratchian, H. P.; Cross, J. B.; Bakken, V.; Adamo, C.; Jaramillo, J.; Gomperts, R.; Stratmann, R. E.; Yazyev, O.; Austin, A. J.; Cammi, R.; Pomelli, C.; Ochterski, J. W.; Ayala, P. Y.; Morokuma, K.; Voth, G. A.; Salvador, P.; Dannenberg, J. J.; Zakrzewski, V. G.; Dapprich, S.; Daniels, A. D.; Strain, M. C.; Farkas, O.; Malick, D. K.; Rabuck, A. D.; Raghavachari, K.; Foresman, J. B.; Ortiz, J. V.; Cui, Q.; Baboul, A. G.; Clifford, S.; Cioslowski, J.; Stefanov, B. B.; Liu, G.; Liashenko, A.; Piskorz, P.; Komaromi, I.; Martin, R. L.; Fox, D. J.; Keith, T.; Al-Laham, M. A.; Peng, C. Y.; Nanayakkara, A.; Challacombe, M.; Gill, P. M. W.; Johnson, B.; Chen, W.; Wong, M. W.; Gonzalez, C.; Pople, J. A.; Gaussian, Inc.: Wallingford, CT, 2004.